Water Resources Management
https://doi.org/10.1007/s11269-022-03175-4

Design of a Control System Using an Artificial Neural Network to Optimize the Energy Efficiency of Water Distribution Systems

Laís Régis Salvino[1] · **Heber Pimentel Gomes**[2] · **Saulo de Tarso Marques Bezerra**[3]

Received: 30 June 2021 / Accepted: 4 May 2022

Abstract
Sustainable management of water supply systems is a major challenge within the framework of the water-energy nexus. The main strategies to improve the operation of these systems are related to increasing the hydraulic and energy efficiency of pumping systems. In this context, this work presents a new artificial neural network (ANN) controller to improve the operation of water distribution systems (WDSs) that includes in its algorithm the specific energy consumption (SEC) as a decision parameter. Therefore, pressure control at the measuring points is also based on the energy efficiency of the pumps. The technique was applied to control the pressures in an experimental setup that emulates a WDS with two consumption zones with different topographies. For this purpose, the controller acted on a conventional pump, a booster pump and a control valve. To analyze the performance under the controller action, tests were performed emulating water-demand scenarios, introducing perturbations and changing the pressure setpoints. The real-time control performance was proven based on the dynamic performance, steady-state performance and SEC. The experimental results showed that the proposed controller kept the pressures close to the setpoints and provided a reduction in the SEC between 15.1% and 17.8%, compared with the uncontrolled system, and an economy that varied from 2.5% to 8.1% compared with the performance of the ANN based only on pressure control.

Keywords Water supply · Real-time control · Pressure control · Energy efficiency · Artificial neural network

✉ Saulo de Tarso Marques Bezerra
saulo.tarso@ufpe.br

Laís Régis Salvino
laissalvino13@gmail.com

Heber Pimentel Gomes
heberp@uol.com.br

[1] Laboratory of Energy and Hydraulic Efficiency in Sanitation, Federal University of Paraiba, João Pessoa, Paraíba, Brazil

[2] Department of Civil and Environmental Engineering, Federal University of Paraiba, João Pessoa, Paraíba, Brazil

[3] Department of Technology, Federal University of Pernambuco, Caruaru, Pernambuco, Brazil

Published online: 16 May 2022

1 Introduction

Sustainable management of water distribution systems (WDSs) is becoming a major challenge within the framework of the water-energy nexus. Reduced water loss and an efficient use of energy are considered essential to contain environmental impacts and the high operational costs of the WDSs. Water utilities use 0.4–2.3% of primary energy or 0.6–6.2% of regional electricity (Kenway et al. 2019), while 80–90% of this consumption is absorbed by motor-pump sets (Moreira and Ramos 2013).

According to Zhang et al. (2012) and Carravetta et al. (2017), the main strategies to increase the energy efficiency of WDSs are related to increasing the hydraulic efficiency of the pumps and the electrical efficiency of motors, introducing performance standards to which the pumps on the market must comply, assessing energy use in the network and using variable frequency drives (VFDs) to increase the efficiency of pumping systems operating in variable conditions.

In addition to reducing energy consumption, VFDs can increase the hydraulic efficiency of WDSs through pressure management. Pressure control has the following benefits: increases the useful life of the pipes, increases the reliability of the facilities, reduces hydraulic transients, reduces water consumption and reduces the volume of water losses. Koor et al. (2016) proposed an algorithm running variable-speed pumps (VSP) working in parallel to keep them running close to the best efficiency point provided by the manufacturer. The authors solved the complex optimization task to maximize the total efficiency of pumping systems, and thereby minimize energy consumption.

To solve the problem of poor quality and wasted electric energy of a direct pump, Peng et al. (2009) introduced a constant pressure in a WDS, adopting embedded fuzzy control technology using a programmable logic controller (PLC) and VFD. Comparing the value of measured pressure with its setpoint value, the PLC controls the power supply frequency by the output signal on fuzzy calculation to control the rotation speed of the pump and adjust the pressure. The real-time control (RTC) performance was appropriate according to the experimentation validated. The hardware module was steady and reliable, and the fuzzy controller was valid and able to guarantee better stability in water pressure. Hongfeng et al. (2009) and Ding and Cao (2010) performed comparative analyses between the fuzzy PID (proportional-integral-derivative) controller and the conventional PID controller to maintain a constant pressure in a WDS. Taking the pump as the load of the asynchronous motor allowed the whole system to be simplified as a second-order model. Comparisons were made in terms of dynamic performance, steady-state performance and noise immunity. The simulation results showed that the fuzzy PID controller not only had a faster response, slighter overshoot and stronger noise immunity, but also a wider adaptation range and higher accuracy in stability than the PID controller.

Among the first research that investigated the RTC for pressure control in WDS were the proportional algorithms presented by Campisano et al. (2012, 2016). Campisano et al. (2012, 2016) reported the results of a numerical investigation aimed at assessing the effectiveness of valve control in reducing leakage in WDSs. They programmed logic units using proportional algorithms, which regulated the closure settings of the valves by pressure measurements carried out at appropriate control nodes.

Creaco et al. (2019) presented a review of the current state-of-the-art RTC of water distribution systems. The researchers presented basic concepts related to RTC in addition to sensors, actuator devices and controllers commonly used in WDSs. The work also provides a perspective of potential future developments in this area.

In practice, it is common to apply PID control techniques in WDS pumping systems and control valves. Designing and tuning these controllers appears to be conceptually intuitive but can be hard in practice if multiple (and often conflicting) objectives, such as short transience and high stability, are to be achieved. However, in some specific cases, a WDS cannot undergo major changes in its operation conditions (e.g., the operation of fire hydrants or a break of a transmission main), with the risk that the control will become unstable or require adjustments to its parameters. Besides that, if a large time delay is not correctly considered, then oscillations and instabilities in the control process can occur in controlling the pump rotation in large WDSs (Moura et al. 2018; Moreira et al. 2021).

Neural network controllers have been highlighted due to their degree of applicability and can be used in complex dynamic systems with multiple variables. Depending on the configuration and type of algorithm, these controllers can be used for forecasting, optimization and process control.

Artificial neural networks (ANNs) can be described as nonlinear mathematical techniques designed by simulation of biological nervous systems (Vaferi et al. 2016). In other words, ANNs are a rough approximation and simplified simulation of biological neural networks (Islam et al. 2020). ANNs have been applied in almost all branches of science (Meshram et al. 2021), including agricultural (Ravindran et al. 2021; Sharifi et al. 2021), environment (Scheres and Van der Putten 2017; Sekertekin et al. 2020), geology (Pham et al. 2017; Mandal and Mondal 2019), hydrology (Sharghi et al. 2018; Wu et al. 2021), and water supply (Vijay and Kamaraj 2021; Wadkar et al. 2021).

Antsaklis and Passino (1989) and Narendra and Parthasarathy (1990) presented one of the first studies on the use of this technique for intelligent process control. Narendra and Parthasarathy (1990) demonstrated that neural networks can be used effectively to identify and control nonlinear dynamic systems. The authors presented models of networks with multiple layers and recurrent, with a static and dynamic backpropagation method for parameter adjustment.

Barros Filho et al. (2018) and Moura et al. (2018) developed intelligent controllers based on ANNs for water supplies. The purpose of the controllers was to automate the process and define the operating state of the variable-speed pumps. The systems developed were generic, which allowed the application of their control structure in similar processes, and they were applied in an experimental setup that emulated real systems. Results showed excellent performance in terms of pressure regulation.

The development of controllers for WDSs is mainly intended to regulate the pressure at the measurement points, the distributed flow or the control of tank filling, disregarding the search for the best operating point of the pumps in the process. The inclusion of specific energy consumption (SEC) as a decision parameter in the proposed controller algorithm is an innovation presented in this work, as it allows the control of the pump rotation speed to be based on the energy efficiency of the system, as well. The SEC was adopted to evaluate the performance of the system because it is an efficiency indicator widely used by utility managers.

This paper presents a new adaptive ANN controller for the pressure control of water distribution systems with pumps and valves acting simultaneously.

2 Experimental Setup

The implementation of the experimental setup (Fig. 1) was intended to display a quantitative assessment of savings from the energy efficiency point of view with respect to a conventional operation. It emulated a real WDS with two consumption zones with different

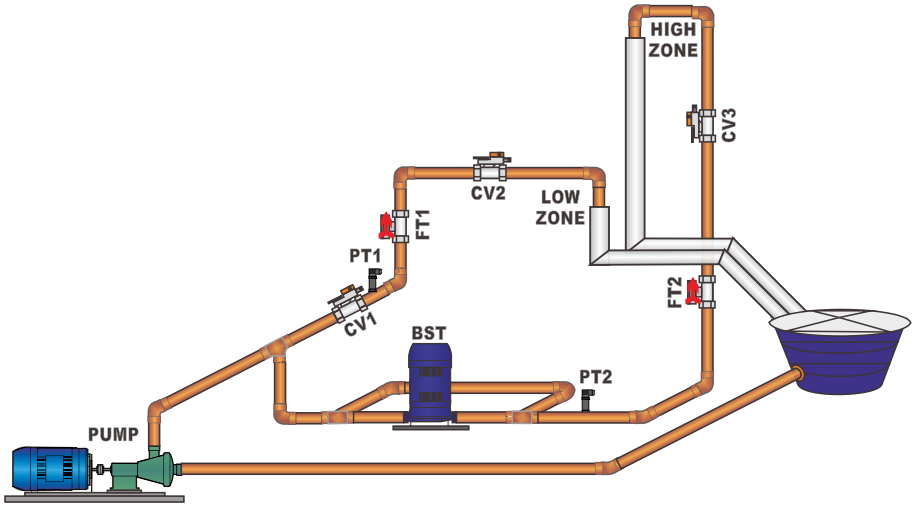

Fig. 1 Schematic diagram of experimental setup

topographies. The system was powered by a pumping system (PUMP) connected to a reservoir, consisting of a three-phase 3 HP induction motor, a Schneider pump model BC-21R and a KSB booster pump (BST) model Megaline to improve the hydraulic head in the high zone. The pumping systems were driven by two independent variable frequency drives (VFDs). In this way, it was possible to control the rotation speed of the pumps separately.

Two control valves (CV2 and CV3) were used to vary the demands at the consumption points of the experimental setup. These valves were located in the discharge branches of the Low Zone (LZ) and High Zone (HZ), respectively. Upstream of the LZ, a control valve (CV1) was installed, which acted as a pressure-reducing valve.

LabVIEW, a graphical programming language to accommodate the SCADA system in a microcomputer, was used as data acquisition and instrument control software. It allowed an operator to change setpoints on the controller, open/close valves, monitor alarms and to gather instrument information from a local process to a widely distributed process. The system was constructed in a microcomputer with two data acquisition modules (USB-6221 and USB-6229) manufactured by National Instruments. The PC used in the experiments had an Intel Core i7 with 8 GB of main memory.

The data acquisition network was designed to characterize the system performance. For this purpose, a network of sensors was set up to monitor the most relevant parameters of the system. These sensors measured pressure (PT1 and PT2), flow (FT1 and FT2) and power consumption. The pressure sensors were Acros TP-ST18 with accuracy $\pm 0.25\%$ FS. The flow meters were Incontrol, model VMS 038 6000 with accuracy $\pm 0.5\%$ FS.

3 Artificial Neural Network Controller

The developed controller, which uses an ANN with backpropagation learning, was applied to the experimental setup to control the pressure at the measurement points PT1 and PT2 and to minimize the SEC of the pumps.

The inclusion of this indicator in the controller algorithm is an innovation in the formulation of control systems for WDSs. An ANN with backpropagation learning is the most common one used in dynamic systems for optimization, identification and control of processes.

ANNs are collections of small, individually interconnected processing units. Information is passed between these units along interconnections; the incoming connection has two values associated with it, an input value and a weight. The node receives weighted activation of other nodes through its incoming connections. First, these are added up (summation). The result is then passed through an activation function and transferred to the next node. A neural network consists of many nodes joined together, usually organized in groups called layers. A typical network consists of a sequence of layers with full or random connections between successive layers (typically two layers with connections to the outside world): an input buffer where data is presented to the network, and an output buffer that holds the response of the network to a given input pattern. Layers distinct from the input and output buffers are called hidden layers, and in principle, there could be more than one hidden layer. In such a system, excitation is applied to the input layer of the network (Hasan et al. 2006).

The proposed model was an ANN composed of an input layer, a hidden layer and the output layer. Recently, researchers showed that a three-layered ANN using the back-propagation algorithm can approximate any well-behaved nonlinear function to any desired degree of accuracy (Funahashi 1989). The input layer had seven neurons: pressure in the LZ (PT1), flow pumped into LZ (FT1), pressure in the HZ (PT2), flow pumped into the HZ (FT2), delay of the control signal of the PUMP frequency. (PUMP(t-1)), delay of the control signal of the CV1 ($CV1_{(t-1)}$) and delay of the control signal of the BST frequency ($BST_{(t-1)}$). The activation function in this layer was linear. The middle layer had seven neurons (experimentally defined quantity) and, due to the nonlinearity of the neurons present in this layer, the activation function used was the hyperbolic tangent function. Figure 2 presents the block diagram of the system.

To minimize the SEC and simultaneously control the pressures in the zones, the controller acted on the experimental setup actuators, which were the VFD that drove the pumps (PUMP and BST) and the control valve (CV1). The ANN also had a neuron in the output layer for each actuator. Figure 3 shows the architecture of the ANN controller, where it is possible to observe the various elements of real-time operation and training of the network.

The ANN and the design steps of the control system are described as follows. Steps 3 to 7 refer to the operation phase (forward pass), which covers the steps of calculating the output signals of the intermediate-layer neurons and the output signals of the network.

- **Step 1:** Triggering the experimental setup. The initial value of the activation power-supply frequency of the pumping systems was set at 0 Hz and the valve closing angle at 0º (fully open).
- **Step 2:** Controller activation. The input layer of the ANN received the values of pressure, flow, power supply frequency and valve closing angle in real time.
- **Step 3:** The input layer signals were calculated by Eqs. (1) and (2). Weighting was performed using the synaptic weight matrix, which received random values between -1 and 1 in the first iteration. In this step, the activation threshold (or bias) received a random value between 0 and 1.

$$\left\{x_{E_1}, x_{E_2}, \ldots, x_{E_7}\right\} = \left\{y_{E_1}, y_{E_2}, \ldots, y_{E_7}\right\} \tag{1}$$

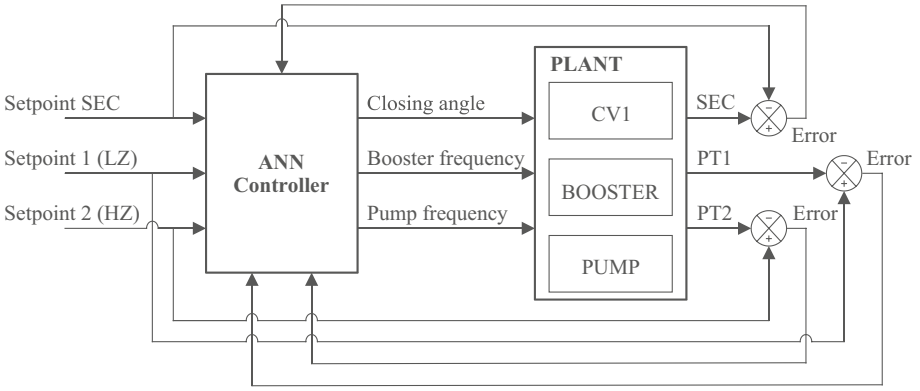

Fig. 2 Block diagram of the system

$$\left\{x_{I_1}, x_{I_2}, \ldots, x_{I_7}\right\} = \left\{y_{E_1}, y_{E_2}, \ldots, y_{E_7}\right\} \cdot \begin{bmatrix} w_{I_{11}} & w_{I_{12}} & \cdots & w_{I_{17}} \\ w_{I_{21}} & \ddots & \cdots & \vdots \\ \vdots & \vdots & \ddots & \vdots \\ w_{I_{71}} & \cdots & \cdots & w_{I_{77}} \end{bmatrix} - \left\{\beta_1, \beta_2, \ldots, \beta_7\right\} \quad (2)$$

where $w_{I_{77}}$ represents the matrix of synaptic weights, whose elements denote the value of the synaptic weight connecting the neurons of the input layer with the neurons of the intermediate layer; y_E is the vector of the output signals from the neurons of the input layer; and

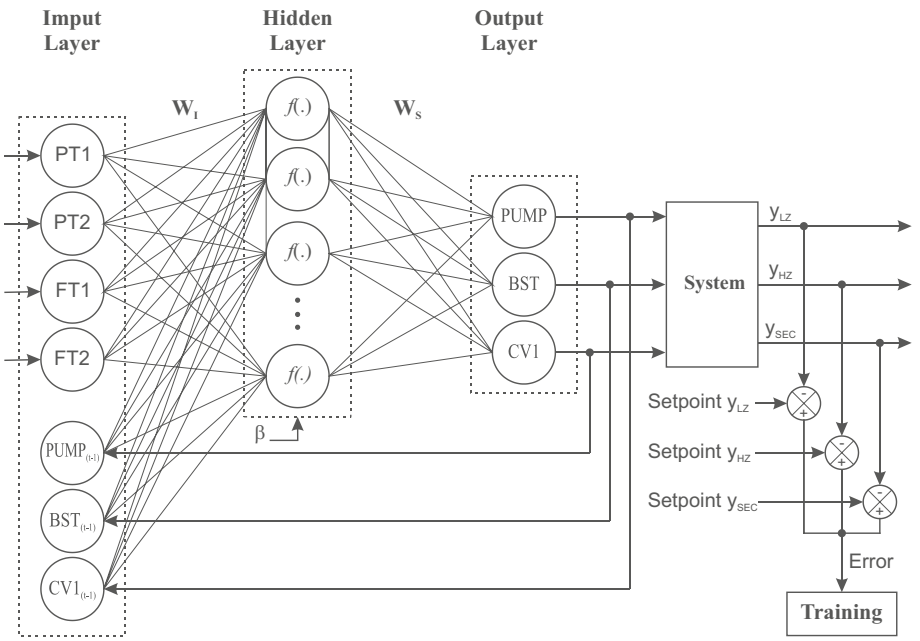

Fig. 3 Artificial Neural Network architecture

β_{I_7} is the vector of the activation threshold (or bias) present in the neurons of the intermediate layer.

- **Step 4:** The output signals from neurons that belong to the middle layer were calculated by Eq. (3).

$$y_{I_k} = f\left(x_{I_k}\right) = \frac{1 - e^{-\varphi_{I_k} x_{I_k}}}{1 + e^{-\varphi_{I_k} x_{I_k}}} \tag{3}$$

where y_{I_k} is the activation function of neurons belonging to the middle layer of the ANN. For this work, the activation function was the hyperbolic tangent with an interval between the values -1 and 1, and φ_{I_k} is the parameter of the activation function.

- **Step 5:** The signals coming out of the middle layer (input signals from the neurons in the output layer, x_{S_l}) were weighted by the synaptic weight matrix W_S (Eq. (4)).

$$x_{S_l} = \left\{y_{I_1}, y_{I_2}, \ldots, y_{I_7}\right\} \cdot \begin{bmatrix} w_{S_{11}} & w_{S_{12}} & \cdots & w_{S_{17}} \\ w_{S_{21}} & \ddots & \vdots & \vdots \\ \vdots & \vdots & \ddots & \vdots \\ w_{S_{71}} & \cdots & \cdots & w_{S_{77}} \end{bmatrix} \tag{4}$$

- **Step 6:** The weighted signals entered the output layer and passed through a linear activation function, in which the three output signals from that layer (control signals) were calculated. In this case, $w_{S_{mn}}$ is the weight matrix responsible for weighting the values between the neurons of the middle layer and those of the output layer, and y_{I_k} is the output vector of the neurons of the middle layer. The activation function used in calculating the network output was linear and, therefore, the output signals were determined by Eq. (5).

$$y_{S_l} = x_{S_l} = \left\{y_{I_1}, y_{I_2}, y_{I_3}\right\} \cdot \begin{bmatrix} w_{S_{11}} & w_{S_{12}} & \cdots & w_{S_{13}} \\ w_{S_{21}} & \ddots & \vdots & \vdots \\ \vdots & \vdots & \ddots & \vdots \\ w_{S_{71}} & \cdots & \cdots & w_{S_{73}} \end{bmatrix} \tag{5}$$

- **Step 7:** At the end of this iteration, the u_x control signals were sent to the actuators (VFD and CV1). Thus, the controller responded with a y_R signal that represented the actual system response to the control signals. After obtaining y_R, the error (E) was calculated using Eq. (6):

$$E = y_{ref} - y_R \tag{6}$$

The training (backward pass) was carried out in unsupervised learning. In this stage, the error backpropagation algorithm, together with the gradient descent method, adjusted the synaptic weights (Eq. (7)), the activation threshold value (bias) (Eq. (8)) and the function parameter activation code φ_I (Eq. (9)). The adjustment of the weights located between the input and intermediate layers occurred from the application of Eq. (10).

$$w_{S_{77}} = \begin{bmatrix} w_{S_{11}} & w_{S_{12}} & \cdots & w_{S_{13}} \\ w_{S_{21}} & \ddots & \vdots & \vdots \\ \vdots & \vdots & \ddots & \vdots \\ w_{S_{71}} & \cdots & \cdots & w_{S_{73}} \end{bmatrix} + \mu \left(\begin{Bmatrix} E_{S_1} \\ E_{S_2} \\ \vdots \\ E_{S_3} \end{Bmatrix} \cdot \left\{ y_{I_1}, y_{I_2}, \ldots, y_{I_3} \right\} \right) \tag{7}$$

$$\beta_I = \left\{ \beta_1, \beta_2, \ldots, \beta_7 \right\} + \mu \left(\begin{Bmatrix} x_{S_1} \\ x_{S_2} \\ \vdots \\ x_{S_7} \end{Bmatrix} \cdot \begin{bmatrix} w_{S_{11}} & w_{S_{12}} & \cdots & w_{S_{17}} \\ w_{S_{21}} & \ddots & \vdots & \vdots \\ \vdots & \vdots & \ddots & \vdots \\ w_{S_{71}} & \cdots & \cdots & w_{S_{77}} \end{bmatrix} \times \frac{\varphi_{I_k}}{2} \left[1 - {y_I}^2 \right] \right) \tag{8}$$

$$\varphi_I = \left\{ \varphi_1, \varphi_2, \ldots, \varphi_7 \right\} + \mu \left(\begin{Bmatrix} E_{S_1} \\ E_{S_2} \\ \vdots \\ E_{S_3} \end{Bmatrix} \cdot \begin{bmatrix} w_{S_{11}} & w_{S_{12}} & \cdots & w_{S_{17}} \\ w_{S_{21}} & \ddots & \vdots & \vdots \\ \vdots & \vdots & \ddots & \vdots \\ w_{S_{71}} & \cdots & \cdots & w_{77} \end{bmatrix} \times \frac{x_I}{2} \left[1 - {y_I}^2 \right] \right) \tag{9}$$

$$w_I = \begin{bmatrix} w_{I_{11}} & w_{I_{12}} & \cdots & w_{I_{17}} \\ w_{I_{21}} & \ddots & \vdots & \vdots \\ \vdots & \vdots & \ddots & \vdots \\ w_{I_{71}} & \cdots & \cdots & w_{S_{77}} \end{bmatrix} + \mu \left(\begin{Bmatrix} E_{S_1} \\ E_{S_2} \\ \vdots \\ E_{S_3} \end{Bmatrix} \cdot \begin{bmatrix} w_{S_{11}} & w_{S_{12}} & \cdots & w_{S_{17}} \\ w_{S_{21}} & \ddots & \vdots & \vdots \\ \vdots & \vdots & \ddots & \vdots \\ w_{S_{71}} & \cdots & \cdots & w_{S_{77}} \end{bmatrix} \times \frac{\varphi_I}{2} \left[1 - {y_I}^2 \right] x_I \right) \tag{10}$$

where μ is the coefficient that represents the network learning rate and E_S is the error, which is equal to the difference generated between the network's output value and the setpoint.

4 Analysis Procedure

To validate the ANN controller, the following parameters were calculated: maximum overshoot, settling time and steady-state error. The overshoot is defined as the difference between the maximum value of the response curve and the steady-state error. The time required for the response curve to reach values within an error range (usually 2–5%) in relation to the steady-state value is defined as settling time. The steady-state error is the difference between the steady-state output and the setpoint.

The system energy performance was analyzed based on the instantaneous measurements of flow and power consumption of its components. The electric consumption parameter was calculated by integrating the power consumption W(t) of different components in the Δt interval (Eq. (11)) numerically. This quantity was calculated for each of the pumping systems with separate power consumption readings. There were two power consumption readings in the experimental setup. The consumption of the PUMP, while the second was the consumption of the BST. For each component, this quantity represented the energy consumed in the Δt interval.

$$W = \int_{To}^{To+\Delta t} W(t)dt \tag{11}$$

The specific energy consumption (SEC) was defined as the ratio between the power consumption W(t) and the total flow pumped in the Δt interval starting at T_0 time (Eq. (12)).

$$SEC = \frac{W}{Vol} \tag{12}$$

5 Experimental Results

The performance of the ANN controller was assessed under three operating conditions: change in water demand (Experiment 1), disturbances in the plant (Experiment 2) and changes in pressure setpoints (Experiment 3).

5.1 Experiment 1

Experiment 1 was intended to evaluate the performance of the ANN controller. The tests started with the condition of the maximum water demand and the closing angle of CV2 and CV3 at 40º. Subsequently, this angle increased by 2º every 30 s until reaching 60º, which corresponded to the minimum demand. Experiment 1 was divided into the three tests:

- **Experiment 1a:** The purpose of this test was to verify the behavior of the experimental setup without the controller acting, thus emulating what happens in a real WDS without pressure control. Then, the pumping systems were activated at the nominal frequency (60 Hz) and the CV1 was kept fully open. The results are shown in Fig. 4a.
- **Experiment 1b:** The test was carried out under the same operating conditions as Experiment 1a (variation in water demand), but with the ANN controller acting on the system. The actuators (PUMP, BST and CV1) were activated by the controller to maintain the pressure in the Low Zone (LZ) at 10 m and the High Zone (HZ) at 15 m. The results are shown in Fig. 4b. At 21 s, there was a maximum overshoot of 34.5% (13.4 m) in the LZ and 2.5% (15.4 m) in the HZ. The settling time for the two con-

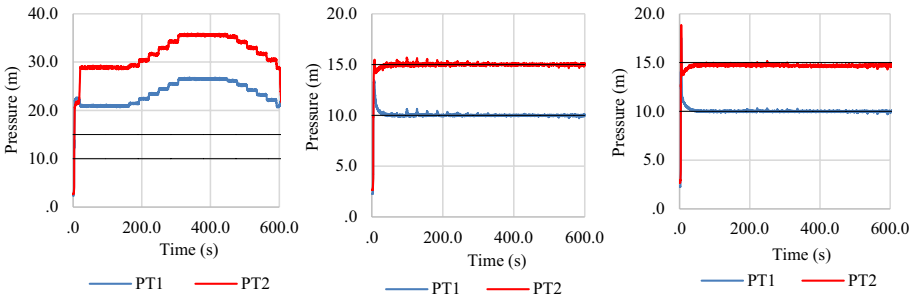

a) Experiment 1a (without the controller acting)

b) Experiment 1b (without the controller acting)

c) Experiment 1c (controller acting for energy efficiency)

Fig. 4 Pressure behaviors at the measuring points

sumption zones in this initial phase was approximately 17 s. The steady-state error was within a range of 0.05 m for the HZ, and 0.03 m for the LZ.

- **Experiment 1c:** This experiment followed the same methodology described in Experiment 1b. However, in addition to controlling the pressure in the two zones, the controller was used to minimize the SEC, whose setpoint was 0 (zero) kWh/m^3. In addition to controlling the pressure, the main purpose of this experiment was to increase the system's energy efficiency. Pressure behaviors at the measuring points are shown in Fig. 4c.

The behavior of the control variables of the system is shown in Fig. 5a. At the beginning controller's performance, the PUMP frequency reached a level close to the nominal and the BST reached 39 Hz. The rapid increase in frequency occurred because the controller was acting to reduce the large difference between the pressure values and the setpoints in the two zones. When the pressure got closer to the reference value, the change in frequencies decreased. As expected, the high frequency values corresponded to the intervals at which the water demand was maximum, while the lowest values represented periods when the demand was minimal. The performance of the controller caused CV1 to reach a 21.6º closing angle and remain so throughout the test.

Figure 5b shows the behavior of the control variables in Experiment 1c. The PUMP frequency reached 53 Hz, while for the BST, this value was 32 Hz. The actuation of the controller on the valve caused its closing angle to vary from 0º to 23.6º. It is worth mentioning that CV1 caused a loss of pressure that affected the pressure reduction downstream of the installation (LZ) and created an increase in pressure upstream, benefiting the HZ.

In Experiment 1b, when the ANN controller was activated, the PT1 pressure reached the setpoint in the LZ in 22 s. The overshoot calculated was 75.3% (17.5 m) and the average steady-state error was 0.29 m. Due to the condition of minimization of the SEC (Experiment 1c), the pressure in this zone did not reach the setpoint in the HZ, accounting for a steady-state error of approximately 0.03 m. The error is acceptable, as there was a significant increase in the energy efficiency of the pumping systems.

5.2 Experiment 2

Experiment 2 was intended to analyze the performance of the ANN controller when subjected to disturbances in the plant. After the system stabilized, disturbances were imposed

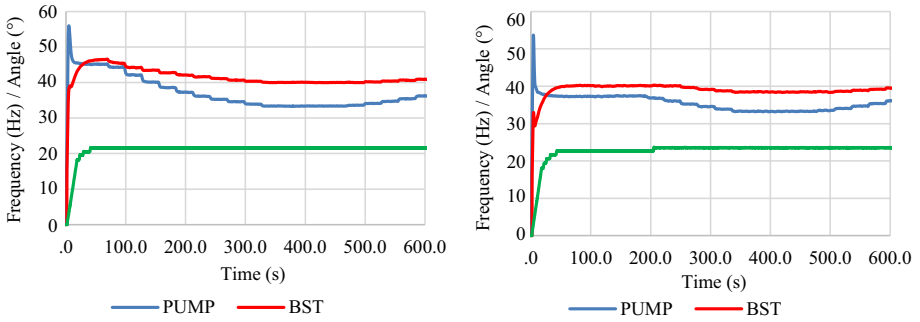

Fig. 5 Behavior of the control variables

on both branches by momentarily closing the valves. In all tests, the measurement points were 10 m (LZ) and 15 m (HZ).

- **Experiment 2a:** The tests were carried out for the condition of minimum water demand in the consumption zones, and the closing angle of CV2 and CV3 remained at 60°. Figure 6a shows the pressure behaviors at the measuring points. As the ANN had its weights previously calculated, there was a decrease in the settling time and no overshoot. The graph shows that the pressures reached the setpoint in a few seconds. The steady-state error for the two consumption regions remained within a range of 0.2 m.
- **Experiment 2b:** The experimental setup was subjected to the same disturbances as Experiment 2a, but with the maximum water demand in the consumption zones. The pressure behaviors of the measuring points are presented in Fig. 6b. As in Experiment 2a, the performance of the ANN controller was satisfactory and the pressures equaled the setpoints in the two zones. The average error was 0.2 m.

5.3 Experiment 3

The tests of Experiment 3 allowed us to verify the accuracy of the ANN controller when subjected to changes in the setpoint. Initially, the reference values were 10 m and 15 m for the LZ and HZ, respectively. Then, different setpoint values were imposed on the system for the measurement points. The results are shown in Fig. 7. The ANN controller proved to be robust, as the steady-state error did not exceed 0.2 m. Additionally, when changing the setpoint of one consumption zone, there were disturbances in the other supplied zone.

Figure 8 shows the behavior of the control variables (PUMP frequency, BST frequency and CV1 angle), in addition to the closing angle of CV2 and CV3. At 4 s, when the controller was activated, the PUMP and the BST frequencies went to 52 Hz and 32 Hz, respectively, intended to quickly reduce the difference between the measured pressures and the setpoints. Whenever the reference pressure was changed in the consumption zones, an adjustment was noticed in the three control variables.

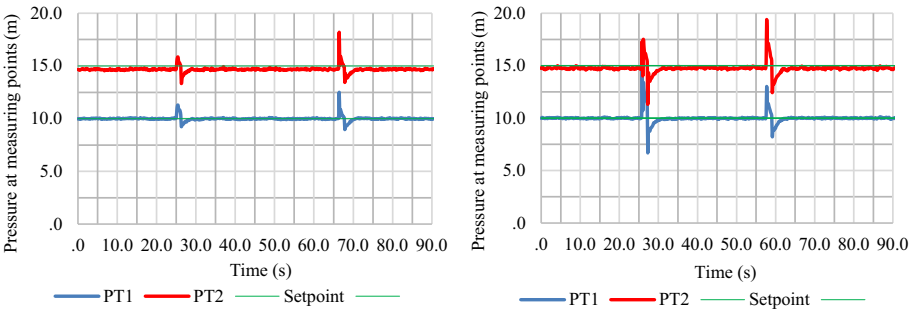

a) Experiment 2a **b)** Experiment 2b

Fig. 6 Pressure behaviors at the measuring points with the controller acting

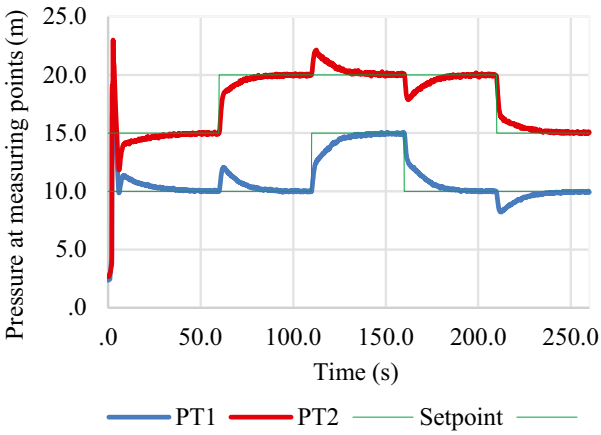

Fig. 7 Pressure behaviors at the measuring points with the controller acting for energy efficiency – Experiment 3

6 Discussions

The results demonstrate the potential for the controller's application to increase systems' hydraulic and energy efficiency. Although the system adopted for the experimental tests is relatively simple compared to complex WDSs, the controller is expected to adapt well to real operating conditions.

As expected, Experiment 1 showed that the controller with the SEC showed greater energy efficiency than the others. For the maximum demand (0–50 s), this provided a reduction in specific consumption of 17.8% and 2.5% in relation to Experiments 1a and 1b, respectively. For minimum water demand (345–400 s), the SEC savings were 2.5% and 15.1%. The time required to converge to the setpoint was not affected by the inclusion of SEC in the controller algorithm, the value remained below 20 s in all tests. This demonstrates the potential for application in real WDS, where changes in water demand are generally much slower.

The controller performance analysis included the evaluation of the system's accuracy in converging to the setpoints. Experiment 2 confirmed that the controller performed well when subjected to disturbances in the plant. These presented an average error of 0.2 m,

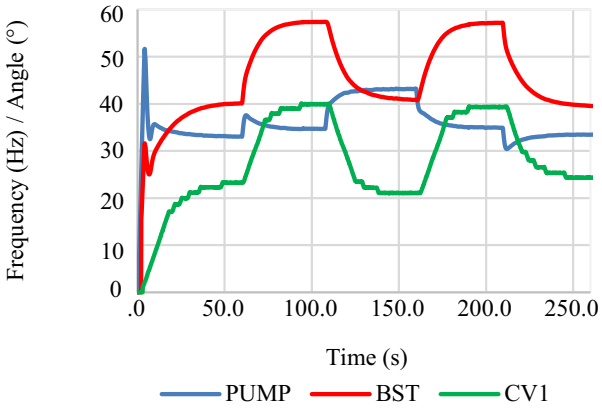

Fig. 8 Behavior of the control variables – Experiment 3

compatible with values described in other works. Barros Filho et al. (2018) and Moura et al. (2018) obtained similar absolute errors (measured value versus setpoint). The first work obtained a maximum error of 2.9% (0.45 m), while the second, for a setpoint of 12.5 m, obtained a maximum error of 1.52% (0.19 m).

The results of Experiment 3 (Fig. 7) show that the plant is coupled, that is, that adjustments made in one of the zones interfere in the other and vice versa. This fact demonstrates the complexity of the simultaneous pressure control of the measurement points in the experimental setup and reinforces the need to develop more robust control systems. The controller maintained good performance when subjected to different setpoints, which confirms the robustness and effectiveness of the proposed control approach.

7 Conclusions

The main objective of this work was to design an ANN with backpropagation learning to autonomously control the pressure in WDSs while increasing the energy efficiency of the pumping systems. Once the setpoints of the pressure measurement points were registered, the ANN controller adjusted the power supply frequency of the motors and the control valves of the system, without the need for manual commands from the operators. In addition, it is noteworthy that the network was applied directly, that is, all training was in real time.

The pressure control and energy efficiency increase in the experimental configuration was applied by adjusting the opening/closure of a valve and the rotation speed of a conventional pump and a booster pump in real time. To assess the performance of the ANN, it was applied in three experiments. Effective pressure control on the experimental setup was observed in all tests. The results confirm the robustness and effectiveness of the proposed control approach. The controller had quick responses, with a settling time of less than 22 s, and the tests did not show an overshoot after ANN training. Errors remained in a range of less than 0.3 m.

Traditionally, the development of controllers for WDSs is mainly intended to regulate pressure at the measurement points, the distributed flow or the control of tank filling. In this work, including SEC in the controller allowed the pumping system to improve its energy efficiency. The experimental results demonstrated a reduction in specific consumption between 15.1% and 17.8% compared with the uncontrolled system, and an economy that varied from 2.5% to 8.1% compared with the performance of the ANN based only on pressure control.

A gap in this work and in the literature is that researchers need to clarify which of the available controllers (fuzzy, neuro-fuzzy etc.) has the best performance. Furthermore, the number of works reporting about experimental results in complex WDSs is very small.

Finally, in line with other recent research applying neural controllers, it is hoped that the developed controller can be applied to real WDSs, mainly due to the ANN's real-time learning ability. The application of the controller can make it possible to reduce water losses in large systems by controlling pressure in addition to increasing energy efficiency.

Authors Contributions All authors contributed to the study conception and design. Material preparation, data collection and analysis were performed by authors. The first draft of the manuscript was written by LRS and all authors commented on previous versions of the manuscript. All authors read and approved the final manuscript.

Funding This research was supported by Centrais Elétricas Brasileiras SA (Eletrobras), Brazilian National Council of Technological and Scientific Development (CNPq) and Coordination for the Improvement of Higher Education Personnel (CAPES) [Financial Code 001].

Data Availability The data will be available upon reasonable request.

Declarations

Ethical Approval This article does not contain any studies with human participants or animals performed by any of the authors.

Consent to Participate The authors agree to participate in the journal.

Consent to Publish The authors agree to publish in the journal.

Competing Interests The authors declare no conflict of interests.

References

Antsaklis PJ, Passino KM (1989) Towards intelligent autonomy control systems: Architecture and fundamental issues. J Intell Rob Syst 1:315–342. https://doi.org/10.1007/BF00126465

Barros Filho EG, Salvino LR, Bezerra STM, Salvino MM, Gomes HP (2018) Intelligent system for control of water distribution networks. Water Sci Technol Water Supply 18(4):1270–1281. https://doi.org/10.2166/ws.2017.188

Campisano A, Modica C, Reitano S, Ugarelli R, Bagherian S (2016) Field-oriented methodology for real-time pressure control to reduce leakage in water distribution networks. J Water Resour Plan Manag 142(12):04016057. https://doi.org/10.1061/(ASCE)WR.1943-5452.0000697

Campisano A, Modica C, Vetrano L (2012) Calibration of proportional controllers for the RTC of pressures to reduce leakage in water distribution networks. J Water Resour Plan Manag 138(4):377–384. https://doi.org/10.1061/(ASCE)WR.1943-5452.0000197

Carravetta A, Antipodi L, Golia U, Fecarotta O (2017) Energy saving in a water supply network by coupling a pump and a pump as turbine (PAT) in a turbopump. Water 9(1):62. https://doi.org/10.3390/w9010062

Creaco E, Campisano A, Fontana N, Marini G, Page PR, Walski T (2019) Real-time control of water distribution networks: A state-of-the-art review. Water Res 16:517–530. https://doi.org/10.1016/j.watres.2019.06.025

Ding C, Cao L (2010) Self-adaptive fuzzy PID controller for water supply system. In Proceedings of the 2010 International Conference on Measuring Technology and Mechatronics Automation – Volume 3, IEEE, pp 311–314. https://doi.org/10.1109/ICMTMA.2010.421

Funahashi KI (1989) On the approximate realization of continuous mappings by neural networks. Neural Netw 2(3):183–192. https://doi.org/10.1016/0893-6080(89)90003-8

Hasan AT, Hamouda AMS, Ismail N, Al-Assadi HMAA (2006) An adaptive-learning algorithm to solve the inverse kinematics problem of a 6 DOF serial robot manipulator. Adv Eng Softw 37(7):432–438. https://doi.org/10.1016/j.advengsoft.2005.09.010

Hongfeng L, Zhenfei C, Wei C (2009) Research of network pressure-superposed water supply system based on Fuzzy-PID controller. In Proceedings of the 2009 IEEE International Conference on Robotics and Biomimetics, IEEE, pp 1194–1199. https://doi.org/10.1109/ROBIO.2009.5420842

Islam J, Vasant PM, Negash BM, Laruccia MB, Myint M, Watada J (2020) A holistic review on artificial intelligence techniques for well placement optimization problem. Adv Eng Softw 141:102767. https://doi.org/10.1016/j.advengsoft.2019.102767

Kenway SJ, Lam KL, Stokes-Draut J, Sanders KT, Binks AN, Bors J, Head B, Olsson G, McMahon JE (2019) Defining water-related energy for global comparison, clearer communication, and sharper policy. J Clean Prod 236:117502. https://doi.org/10.1016/j.jclepro.2019.06.333

Koor M, Vassiljev A, Koppel T (2016) Optimization of pump efficiencies with different pumps characteristics working in parallel mode. Adv Eng Softw 101:69–76. https://doi.org/10.1016/j.advengsoft.2015.10.010

Mandal S, Mondal S (2019) Artificial neural network (ANN) model and landslide susceptibility. In Statistical approaches for landslide susceptibility assessment and prediction. Springer, Cham, pp 123–133. https://doi.org/10.1007/978-3-319-93897-4_5

Meshram SG, Pourghasemi HR, Abba SI, Alvandi E, Meshram C, Khedher KM (2021) A comparative study between dynamic and soft computing models for sediment forecasting. Soft Comput 25(16):11005–11017. https://doi.org/10.1007/s00500-021-05834-x

Moreira DF, Ramos HM (2013) Energy cost optimization in a water supply system case study. Journal of Energy 620698:1–10. https://doi.org/10.1155/2013/620698

Moreira HAM, Gomes HP, Villanueva JMM, Bezerra STM (2021) Real-time neuro-fuzzy controller for pressure adjustment in water distribution systems. Water Supply 21(3):1177–1187. https://doi.org/10.2166/ws.2020.379

Moura GA, Bezerra STM, Gomes HP, Silva AS (2018) Neural network using the Levenberg-Marquardt algorithm for optimal real-time operation of water distribution systems. Urban Water Journal 15(7):692–699. https://doi.org/10.1080/1573062X.2018.1539503

Narendra KS, Parthasarathy K (1990) Identification and control of dynamical systems using neural network. IEEE Trans Neural Networks 1(1):4–27

Peng X, Xiao L, Mo Z, Liu G (2009) The variable frequency and speed regulation constant pressure water supply system based on PLC and fuzzy control. In Proceedings of the 2009 International Conference on Measuring Technology and Mechatronics Automation, IEEE, pp 910–913. https://doi.org/10.1109/ICMTMA.2009.392

Pham BT, Bui DT, Prakash I, Dholakia MB (2017) Hybrid integration of multilayer perceptron neural networks and machine learning ensembles for landslide susceptibility assessment at Himalayan Area (India) using GIS. Catena 149:52–63. https://doi.org/10.1016/j.catena.2016.09.007

Ravindran SM, Bhaskaran SKM, Ambat SKN (2021) A deep neural network architecture to model reference evapotranspiration using a single input meteorological parameter. Environ Process 8(4):1567–1599. https://doi.org/10.1007/s40710-021-00543-x

Scheres B, Van Der Putten WH (2017) The plant perceptron connects environment to development. Nature 543(7645):337–345. https://doi.org/10.1038/nature22010

Sekertekin A, Arslan N, Bilgili M (2020) Modeling diurnal land surface temperature on a local scale of an arid environment using artificial neural network (ANN) and time series of Landsat-8 derived spectral indexes. J Atmos Solar Terr Phys 206:105328. https://doi.org/10.1016/j.jastp.2020.105328

Sharghi E, Nourani V, Najafi H, Molajou A (2018) Emotional ANN (EANN) and wavelet-ANN (WANN) approaches for Markovian and seasonal based modeling of rainfall-runoff process. Water Resour Manag 32(10):3441–3456. https://doi.org/10.1007/s11269-018-2000-y

Sharifi H, Roozbahani A, Hashemy Shahdany SM (2021) Evaluating the performance of agricultural water distribution systems using FIS, ANN and ANFIS intelligent models. Water Resour Manag 35(6):1797–1816. https://doi.org/10.1007/s11269-021-02810-w

Vaferi B, Eslamloueyan R, Ghaffarian N (2016) Hydrocarbon reservoir model detection from pressure transient data using coupled artificial neural network – Wavelet transform approach. Appl Soft Comput 47:63–75. https://doi.org/10.1016/j.asoc.2016.05.052

Vijay S, Kamaraj K (2021) Prediction of water quality index in drinking water distribution system using activation functions based ANN. Water Resour Manag 35(2):535–553. https://doi.org/10.1007/s11269-020-02729-8

Wadkar DV, Nangare P, Wagh MP (2021) Evaluation of water treatment plant using artificial neural network (ANN) case study of Pimpri Chinchwad Municipal Corporation (PCMC). Sustain Water Resour Manag 7(4):1–14. https://doi.org/10.1007/s40899-021-00532-w

Wu Z, Ma B, Wang H, Hu C, Lv H, Zhang X (2021) Identification of sensitive parameters of urban flood model based on artificial neural network. Water Resour Manag 35(7):2115–2128. https://doi.org/10.1007/s11269-021-02825-3

Zhang H, Xia X, Zhang J (2012) Optimal sizing and operation of pumping systems to achieve energy efficiency and load shifting. Electr Power Syst Res 86:41–50. https://doi.org/10.1016/j.epsr.2011.12.002